

## Quantifying the air quality-CO<sub>2</sub> tradeoff potential for airports



Akshay Ashok, Irene C. Dedoussi, Steve H.L. Yim, Hamsa Balakrishnan, Steven R.H. Barrett\*

Laboratory for Aviation and the Environment, Department of Aeronautics and Astronautics, Massachusetts Institute of Technology, 77 Massachusetts Avenue, Cambridge, MA 02139, United States

### HIGHLIGHTS

- We quantify the CO<sub>2</sub>-air quality tradeoffs of aircraft operations at US airports.
- We identify conditions where reducing CO<sub>2</sub> emissions increases air quality impacts.
- Taxi and takeoff engine operations with fixed and changing thrusts are modeled.
- Airports with high potential for air quality improvements are identified.
- Reducing airport air quality impacts beyond fuel burn minimization may be possible.

### ARTICLE INFO

#### Article history:

Received 3 March 2014

Received in revised form

11 October 2014

Accepted 13 October 2014

Available online 15 October 2014

#### Keywords:

Airports

Aircraft engines

Air quality-CO<sub>2</sub> tradeoff

### ABSTRACT

Aircraft movements on the airport surface are responsible for CO<sub>2</sub> emissions that contribute to climate change and other emissions that affect air quality and human health. While the potential for optimizing aircraft surface movements to minimize CO<sub>2</sub> emissions has been assessed, the implications of CO<sub>2</sub> emissions minimization for air quality have not been quantified. In this paper, we identify conditions in which there is a tradeoff between CO<sub>2</sub> emissions and population exposure to O<sub>3</sub> and secondary PM<sub>2.5</sub> – i.e. where decreasing fuel burn (which is directly proportional to CO<sub>2</sub> emissions) results in increased exposure. Fuel burn and emissions are estimated as a function of thrust setting for five common gas turbine engines at 34 US airports. Regional air quality impacts, which are dominated by ozone and secondary PM<sub>2.5</sub>, are computed as a function of airport location and time using the adjoint of the GEOS-Chem chemistry-transport model. Tradeoffs between CO<sub>2</sub> emissions and population exposure to PM<sub>2.5</sub> and O<sub>3</sub> occur between 2–18% and 5–60% of the year, respectively, depending on airport location, engine type, and thrust setting. The total duration of tradeoff conditions is 5–12 times longer at maximum thrust operations (typical for takeoff) relative to 4% thrust operations (typical for taxiing). Per kilogram of additional fuel burn at constant thrust setting during tradeoff conditions, reductions in population exposure to PM<sub>2.5</sub> and O<sub>3</sub> are 6–13% and 32–1060% of the annual average (positive) population exposure per kilogram fuel burn, where the ranges encompass the medians over the 34 airports. For fuel burn increases due to thrust increases (i.e. for constant operating time), reductions in both PM<sub>2.5</sub> and O<sub>3</sub> exposure are 1.5–6.4 times larger in magnitude than those due to increasing fuel burn at constant thrust (i.e. increasing operating time). Airports with relatively high population exposure reduction potentials – which occur due to a combination of high duration and magnitude of tradeoff conditions – are identified. Our results are the first to quantify the extent of the tradeoff between CO<sub>2</sub> emissions and air quality impacts at airports. This raises the possibility of reducing the air quality impacts of airports beyond minimizing fuel burn and/or optimizing for minimum net environmental impact.

© 2014 Elsevier Ltd. All rights reserved.

### 1. Introduction

Aircraft operations at airports result in fuel burn, CO<sub>2</sub> emissions that contribute to climate change, and other emissions that affect

air quality and human health (Simaiakis and Balakrishnan, 2009). Until recently, efforts to reduce the environmental impacts of surface operations have been coupled to the goal of reducing ground delays. This is based on the understanding that reducing taxi times would reduce fuel burn, which would reduce emissions and thereby reduce air quality and climate impacts. For example, Balakrishnan and Jung (2007) developed an integer programming

\* Corresponding author.

E-mail address: [sbarrett@mit.edu](mailto:sbarrett@mit.edu) (S.R.H. Barrett).

formulation to optimize throughput of airports and minimize delays incurred by taxiing aircraft through taxi re-routing and pushback scheduling. The results showed up to an 18% reduction in average taxi-out time at the Dallas/Fort-Worth International Airport, US. Burgain et al. (2009) proposed a pushback control strategy (“N-control”), showing that such a strategy could reduce average passenger delays by up to 15% during congested conditions. Finally, Ravizza et al. (2013) developed an approach to analyze the tradeoff between taxi time and fuel consumption and computed a Pareto front of fuel-optimal and time-optimal aircraft taxi routes at Zurich Airport, Switzerland.

Additionally, other research studies have had the explicit goal of minimizing aircraft fuel burn and emissions. For example, Simaiakis et al. (2011) developed a pushback rate control strategy and reported 12–15 tonnes of fuel savings during eight four-hour tests of the strategy conducted at Boston Logan Airport, US. Nikoleris et al. (2011) estimated aircraft fuel burn and emissions from taxi operations at the Dallas/Fort Worth International Airport using aircraft position data and assumed thrust levels. Jung et al. (2011) evaluated the reductions in taxi delay, fuel burn and emissions of a departure scheduling algorithm. They found a 66% reduction in departure delay and a ~38% reduction in fuel consumption and hydrocarbon (HC), CO and NO<sub>x</sub> emissions. Finally, King and Waitz (2005) estimated that a takeoff at ~80% thrust decreased aircraft NO<sub>x</sub> emissions by 14.5% relative to a conventional maximum thrust takeoff.

Emissions from fuel combustion in aircraft engines at airports affect ambient PM<sub>2.5</sub> and O<sub>3</sub> concentrations from local (~10 km) to regional (~1000 km) scales (Yim et al., 2013; Ashok et al., 2013), which results in changes in human exposure to these pollutants. Epidemiological evidence indicates that adverse health risks are associated with exposure to PM<sub>2.5</sub> and O<sub>3</sub> (USEPA, 2011; WHO, 2008, 2006). The impact of aviation activity on air quality has been quantified for individual airports (Hsu et al., 2012; Hu et al., 2009; Schürmann et al., 2007; Unal et al., 2005; Westerdahl et al., 2008), landing and takeoff (LTO) aircraft activity in the US (Ashok et al., 2013; Woody et al., 2011) and global aircraft activity (Barrett et al., 2010, 2012). Yim et al. (2013) quantified the annual public health impact of operational mitigation measures at UK airports, and found that use of ground electric power, electrification of ground support equipment, single-engine taxiing and desulfurizing jet fuel together could avert ~60% of premature mortalities per year. Dorbian et al. (2011) estimated an average of ~\$230 in monetized climate and air quality damages per tonne of fuel burn below 3000 ft (i.e. LTO).

Tradeoffs between air quality and climate have been studied in the context of household fuel usage (Bailis et al., 2005; Freeman and Zerriffi, 2012), power plants with carbon capture technologies (Koornneef et al., 2010; Tzimas et al., 2007), and alternative-fueled automobiles and marine vessels (Partanen et al., 2013; Lack et al., 2011; MacLean and Lave, 2000). Aardenne et al. (2009) studied global climate change policies targeted at fuel and technology shifts and energy savings, and assessed the tradeoffs with human health and environmental impacts due to degraded air quality. Barrett et al. (2012) identified a climate-air quality tradeoff predominantly relevant to cruise emissions – that of desulfurizing jet fuel. To the knowledge of the authors, no prior studies have assessed the possibility of a tradeoff between air quality impacts and CO<sub>2</sub> emissions (or climate more broadly) for aircraft surface operations.

The purpose of this paper is to quantify conditions in which there is a tradeoff between aircraft CO<sub>2</sub> emissions and population exposure to secondary PM<sub>2.5</sub> or O<sub>3</sub>. We define a “tradeoff” as where a reduction in one of CO<sub>2</sub> emissions or exposure corresponds to an increase in the other. In the case of primary PM<sub>2.5</sub>, exposure is proportional to emissions and no tradeoffs occur. However,

secondary PM<sub>2.5</sub> contributes to the majority of total PM<sub>2.5</sub> population exposure, as primary PM<sub>2.5</sub> is expected to contribute to ~20% of premature mortalities from US LTO activity in 2018 (Ashok et al., 2013). Tradeoffs can occur when the atmospheric response to emissions, associated with fuel burn and therefore CO<sub>2</sub> emissions, is negative. For example, NO<sub>x</sub> emissions may reduce O<sub>3</sub> under certain conditions due to nonlinear O<sub>3</sub> photochemistry (Seinfeld and Pandis, 2006). Similarly, NO<sub>x</sub> emissions may decrease PM<sub>2.5</sub> based on the availability of ammonia (Ashok et al., 2013). Five commonly-used engine types are selected based on archived aviation activity data, and exposure is computed at 34 airports in the US, accounting for 70% of US aviation LTO fuel burn (Simone et al., 2013). We identify time periods at three-hourly intervals over a year in which a tradeoff between CO<sub>2</sub> emissions (which are directly proportional to fuel burn) and population exposure to PM<sub>2.5</sub> and O<sub>3</sub> exists. Reductions in population exposure due to changes in fuel burn and emissions are also quantified. Airports with relatively high reduction potentials – due to a relatively high magnitude and duration of tradeoff between fuel burn and population exposure – are identified. The results of this paper raise the possibility of reducing the air quality impacts of airports beyond minimizing fuel burn (and so entailing a climate and operating cost tradeoff) or optimizing for minimum net environmental impact (for example, by weighting climate and air quality-related impacts using estimates for monetized environmental damage).

## 2. Methods

In Section 2.1 we describe how aircraft emissions are estimated. Section 2.2 provides an overview of the air quality modeling that is used to quantify population exposure to PM<sub>2.5</sub> and O<sub>3</sub> attributable to aircraft emissions. The tradeoff between CO<sub>2</sub> emissions (directly proportional to fuel burn,  $F$ ) and PM<sub>2.5</sub> and O<sub>3</sub> population exposure ( $P$ ) is defined in Section 2.3. We detail our approach to quantifying the tradeoff at US airports in Section 2.4.

### 2.1. Emissions modeling

The total mass of emissions of species  $i$ ,  $M_i$ , from a given engine can be written as a product of an emission index (EI) (defined in aviation as grams of pollutant emitted per kilogram of fuel burned) and the fuel consumed, i.e.  $M_i = F \cdot EI_i(\dot{m}_f)$ , where the emission index is specific to an engine type and may be a function of the rate of fuel burn,  $\dot{m}_f$ . The rate of fuel burn is approximately proportional to engine thrust (Wey et al., 2006).

We model NO<sub>x</sub>, SO<sub>2</sub>, hydrocarbon (HC) and CO emissions from aircraft engines as they are relevant for the formation of secondary PM<sub>2.5</sub> and O<sub>3</sub>. Emissions are computed using the Aviation Emissions Inventory Code (AEIC) v2.1 (Stettler et al., 2011; Simone et al., 2013), with modifications. Emission indices are estimated according to the Boeing Fuel Flow Method 2 (BFFM2, Baughcum et al., 1996). The BFFM2 method uses engine emission certification data from the International Civil Aviation Organization (ICAO), tabulated in the engine emissions databank (ICAO, 2012). Engines are certified at standard thrust settings of 7%, 30%, 85% and 100%, representing engine operation during the taxi/idle, approach, climb-out and takeoff phases of flight. For an arbitrary thrust setting, the BFFM2 method prescribes a log-linear interpolation for the NO<sub>x</sub> emission index ( $EI_{NO_x}$ ) and a log bi-linear interpolation for  $EI_{HC}$  and  $EI_{CO}$ .  $EI_{SO_2}$  is independent of thrust and is calculated assuming a fuel sulfur content (FSC) of 600 ppm with a S<sup>IV</sup>–S<sup>VI</sup> oxidation efficiency of 2% (Stettler et al., 2011). We apply uncertainty distributions to account for variability and deviations in EIs from the ICAO emissions certification measurements upon which emissions estimates are based (Stettler et al., 2011).

The current work includes changes to emissions modeling at low thrust and modeling the dependence on ambient conditions beyond those presented in Stettler et al. (2011). These are described in Sections 2.1.1 and 2.1.2.

### 2.1.1. Estimation of Els at low thrust

Hydrocarbon and CO emission indices increase as thrust is decreased due to incomplete combustion of jet fuel at relatively low combustion temperatures. The BBFM2 over-predicts CO and HC emissions at thrust settings below the lowest certification measurement (7%) that is available for all engines. Based on new and existing experimental data, Herndon et al. (2012) propose the use of a linear relationship between  $El_{HC}$  and fuel flow rate at thrusts below 7%. In particular, for thrust settings below 7% we adopt their suggested relation of

$$\frac{El_{HC}(\dot{m}_f)}{El_{HC}(\dot{m}_{f7\%})} = 1 - a_{HC}(\dot{m}_f - \dot{m}_{f7\%}), \quad (1)$$

where  $a_{HC} = 52 \text{ s kg}^{-1} \pm 23\%$  is the fuel flow dependence parameter for  $El_{HC}$ . We derive a similar expression for  $El_{CO}$  using the experimental data included in the Appendix A of Herndon et al. (2012), i.e.

$$\frac{El_{CO}(\dot{m}_f)}{El_{CO}(\dot{m}_{f7\%})} = 1 - a_{CO}(\dot{m}_f - \dot{m}_{f7\%}), \quad (2)$$

where  $a_{CO} = 29 \text{ s kg}^{-1} \pm 23\%$  is the fuel flow dependence parameter for  $El_{CO}$ . The uncertainty in the fuel flow dependence parameters includes measurement errors and the spread in observed emission indices (Herndon et al., 2012).

### 2.1.2. Dependence on ambient conditions

The dependence of  $NO_x$  emissions on ambient conditions is modeled according to the BBFM2 method. Ambient temperature, pressure and humidity are used to compute correction factors to the ICAO certification Els, which assume sea level standard atmospheric conditions.

We apply the approach of Herndon et al. (2012) for HC emissions, who find a negative correlation between Volatile Organic Compounds (VOC) emissions and temperature at low thrust (<7%), which is detailed in the Supporting information (SI). No data is available for the influence of ambient temperature on CO emissions at low thrust. We assume the same relative correction factors for CO as for HC, on the basis that ambient temperature influences the combustor inlet and operating conditions (Lyon et al., 1979) and the formation of both pollutants is determined by combustion efficiency.

Using GEOS-5 meteorological data from the NASA Global Modeling and Assimilation Office (GMAO) for the year 2006, El correction factors for ambient conditions at US airports are found to be normally distributed with a standard deviation of 8% for  $El_{NO_x}$  and uniformly distributed between  $\pm 50\%$  for  $El_{HC}$ .

## 2.2. Regional air quality modeling

Air quality impacts are calculated using the adjoint of the GEOS-Chem model (GEOS-Chem Adjoint v33). GEOS-Chem is a tropospheric chemistry-transport model (Bey et al., 2001). It performs transport, gas- and aerosol-phase chemistry, as well as wet and dry deposition calculations. It takes as inputs emissions as well as GEOS-5 meteorological data from the NASA GMAO. The modeling domain applied in this study encompasses the contiguous US: between  $-140^\circ$  and  $-40^\circ$  longitude and  $10^\circ$  and  $70^\circ$  latitude. The

resolution of the horizontal grid is  $0.5^\circ \times 0.666^\circ$  (latitude  $\times$  longitude), with 47 vertical layers up to 80 km. Boundary conditions for the domain are obtained by a GEOS-Chem simulation for the global domain (at  $4^\circ \times 5^\circ$  resolution).

The adjoint model of GEOS-Chem, developed by Henze et al. (2007), is used to compute sensitivities of population exposure to  $PM_{2.5}$  or  $O_3$  to aircraft emissions (Errico, 1997; Henze et al., 2007; Koo et al., 2013). It is based on the forward model described above, and the same grid.

An adjoint model is a computationally efficient way of calculating sensitivities, which are partial derivatives of a quantity of interest with respect to various control parameters. In the present study, annually averaged population exposure to  $PM_{2.5}$  or  $O_3$ , i.e.  $P_{PM_{2.5}}$  or  $P_{O_3}$  are the quantities of interest. They are defined as

$$P_{PM_{2.5}} = \frac{1}{N_{steps}} \sum_{k=1}^{N_{cells}} \sum_{t=1}^{N_{steps}} [p(k) \cdot C_{PM_{2.5}}(k, t)] \quad (3)$$

and

$$P_{O_3} = \frac{1}{N_{steps}} \sum_{k=1}^{N_{cells}} \sum_{t=1}^{N_{steps}} [p(k) \cdot C_{O_3}(k, t)], \quad (4)$$

respectively, where  $k$  indexes GEOS-Chem model surface layer grid cells from 1 to  $N_{cells}$ ,  $t$  indexes model time steps from 1 to  $N_{steps}$ ,  $p(k)$  is the population in grid cell  $k$ ,  $C_{PM_{2.5}}(k, t)$  is the mass concentration (in  $ng/m^3$ ) of  $PM_{2.5}$  at grid cell  $k$  at time interval  $t$ , and  $C_{O_3}(k, t)$  is the mixing ratio (in ppt) of  $O_3$  at grid cell  $k$  at time step  $t$ . The population data was re-gridded from the 30 arc-second resolution data obtained from the GRUMP 2006 database (Balk et al., 2006).

The control parameters in this case are the different aviation emission species,  $M_i$ . Therefore, the sensitivities computed by the nested grid GEOS-Chem adjoint model are

$$S_i(K, T) = \frac{\partial P}{\partial M_i(K, T)}$$

which are computed separately for population exposure to  $PM_{2.5}$  or  $O_3$ . The units of the sensitivities for each time step therefore are  $ppl \text{ ngm}^{-3} \text{ kg}^{-1}$  and  $ppl \text{ ppt kg}^{-1}$  for  $PM_{2.5}$  and  $O_3$  respectively, and quantify the change in population exposure given a change in any of the emission species  $M_i$  at each point in time. Note that in this case  $K$  is the location of emission (an airport) rather than the location of exposure (denoted by  $k$ ), thus the sensitivity is for spatially-integrated exposure to emissions at location  $K$ . Similarly, while  $T$  is the time step of emission,  $t$  in Equations (3) and (4) denotes the time step of exposure. The adjoint sensitivities are calculated relative to an emissions scenario which includes aircraft emissions. We expect that second-order effects caused by aviation emissions on the adjoint sensitivities are negligible (Ashok et al., 2013; Koo et al., 2013). The adjoint simulations were for a 12-month period, with an additional period of 3 months used as the adjoint spin-up time to ensure that the complete impact of the emissions on air quality is captured, assuming that any emission event does not contribute significantly to exposure beyond 3 months after the event. The sensitivities are therefore interpreted as the partial derivatives of annual average total US population exposure with respect to emission of species  $i$  at any time and any location. We use these adjoint-calculated sensitivities to estimate exposure, i.e.

$$P(F, K, T, \dot{m}_f) = \sum_i S_i(K, T) \cdot M_i = F \cdot \sum_i S_i(K, T) \cdot El_i(\dot{m}_f). \quad (5)$$

The sensitivities  $S_i$  are functions of location and time of emissions (in our case, emissions in time interval  $T$  at airport  $K$ ). Thus, population exposure is a function of the total amount of fuel burn ( $F$ ), the location and time of operation ( $K$  and  $T$ ) as well as the thrust setting of the engine (equivalently the fuel burn rate,  $\dot{m}_f$ ), which affects the EI.

### 2.3. Tradeoff between CO<sub>2</sub> emissions and population exposure to PM<sub>2.5</sub> and O<sub>3</sub>

The relationship between population exposure and CO<sub>2</sub> emissions (proportional to fuel burn) is obtained by taking the partial derivative of  $P$  with respect to  $F$  in Eq. (5), to yield.

$$\frac{\partial P}{\partial F} = \sum_i S_i(K, T) \cdot EI_i(\dot{m}_f) \quad (6)$$

The partial derivative denotes the change in population exposure with respect to fuel burn, while holding thrust setting constant for a given time and airport.

Typically we expect the relationship between aviation fuel burn and the resulting exposure to pollutants to be positive. While this assumption may hold true for long-term impacts [for example, as demonstrated by Ashok et al. (2013) and Koo et al. (2013)], hourly atmospheric sensitivities  $S_i$  at a given airport location  $K$  and time of emissions  $T$  may be either positive or negative depending on atmospheric conditions. For example, O<sub>3</sub> formation is dependent on background NO<sub>x</sub> and hydrocarbon concentrations, and under certain conditions aircraft emissions may lead to an O<sub>3</sub> reduction. Similarly, a reduction in sulfate PM<sub>2.5</sub>, one of the main components of PM<sub>2.5</sub>, may occur due to increased NO<sub>x</sub> emissions based on the competition for free ammonia in the atmosphere, as will be explained in Section 3.1.2. Thus, when combined with emissions indices as per Eq. (6), negative atmospheric sensitivities could result in a tradeoff between CO<sub>2</sub> emissions and air quality, i.e.  $\partial P/\partial F < 0$ .

### 2.4. Approach to quantify tradeoffs

We assess the relationship between CO<sub>2</sub> and population exposure to PM<sub>2.5</sub> and O<sub>3</sub> for five commonly-used aircraft engines in the US aircraft fleet. Engines were selected based on activity data obtained from the FAA's Aviation Performance Metrics (APM) database for 2012 for 35 Operational Evolution Partnership (OEP) airports in the US (see Section S3 of the SI). The OEP airports are among the busiest in the US, representing more than 70% of passenger traffic in the US (FAA, 2011). Table 1 lists the engines, their abbreviations used in this paper, and an example aircraft within the US fleet that is powered by the engine.

We evaluate Eq. (6) for every set of atmospheric sensitivities over the course of a year (sampled every 3 h) at all of the OEP airports except Honolulu International Airport, in order to capture spatial and temporal variations in sensitivities. Eight discrete thrust settings are used: 4%, 7%, 10% and 13% to span the range of taxi

thrusts, and 85%, 90%, 95% and 100% to span the range of takeoff thrusts. These thrust settings were selected to reflect operational taxi thrust settings and reduced thrust takeoffs observed at airports, and are based on a review of literature from Stettler et al. (2011) and King and Waitz (2005).

## 3. Results

The analysis method in Section 2.4 results in a four-dimensional "lookup table" of relationships between fuel burn and population exposure indexed by engine type, thrust setting, airport location and time of emissions. As an example, Table 2 shows the change in population exposure to PM<sub>2.5</sub> and O<sub>3</sub> per kilogram fuel burn at Hartsfield-Jackson Atlanta International Airport (ATL), for two of the five engine types, and all eight thrust settings.

The values shown in Table 2 represent the change in population exposure to PM<sub>2.5</sub> and O<sub>3</sub> per kilogram of fuel burn annually averaged and for a single hour. The annually averaged values are positive, implying that a unit of fuel burn every hour of the year causes a net increase in population exposure. However, considering the specific example hour shown, a unit increase in fuel burn causes a decrease in PM<sub>2.5</sub> and O<sub>3</sub> exposures at 7% thrust or higher. We therefore have a tradeoff between the CO<sub>2</sub> and air quality impacts of emissions during these conditions, where minimizing CO<sub>2</sub> emissions leads to an increase in population exposure to PM<sub>2.5</sub> and O<sub>3</sub>, all else held constant.

In Section 3.1 we quantify the total duration of occurrence (over an annual period) of tradeoff conditions. In Section 3.2, we evaluate the magnitude of the tradeoff between CO<sub>2</sub> emissions and population exposure to PM<sub>2.5</sub> and O<sub>3</sub>. Finally, in Section 3.3 we combine the magnitude and duration information to identify airports with relatively high potential for exposure reduction.

### 3.1. Duration of occurrence of CO<sub>2</sub> – air quality tradeoff

#### 3.1.1. Annual duration

The fraction of year for which a CO<sub>2</sub>–air quality tradeoff occurs is given in Fig. 1(a) and (b) for PM<sub>2.5</sub> and O<sub>3</sub> impacts, respectively. At the 4% taxi thrust setting, CO<sub>2</sub> is negatively correlated with PM<sub>2.5</sub> and O<sub>3</sub> population exposure 2–3% and 5–12% of the year, respectively, depending on the engine type, when averaged across all airport locations. At the 100% takeoff thrust setting, the tradeoff duration increases to 14–18% of the year for PM<sub>2.5</sub> exposure, and ~60% of the year for O<sub>3</sub> exposure. For a given thrust setting, variability in annual tradeoff durations across engines arises due to differing emission characteristics amongst engines. For all engines, HC and CO emissions decline with increased thrust while NO<sub>x</sub> emissions increase.

At high (takeoff) thrusts, the occurrence of tradeoff conditions is limited by the presence of negative atmospheric NO<sub>x</sub> sensitivities, i.e. occasions where  $S_{NO_x} = \partial P/\partial M_{NO_x} < 0$ . This is because, as thrust increases, the ratio between  $EI_{NO_x}$  and other species becomes larger. For example for the CFM56 engine, increasing thrust from 4% to 100% increases  $EI_{NO_x}/EI_{HC}$  from ~1/3 to ~256,  $EI_{NO_x}/EI_{CO}$  from ~1/

**Table 1**

Five engines selected for the current study. The engine manufacturer, name, year of certification, ICAO unique identifier (UID) and abbreviation used in this work are tabulated. An example aircraft within the US fleet that is powered by the engine is also listed.

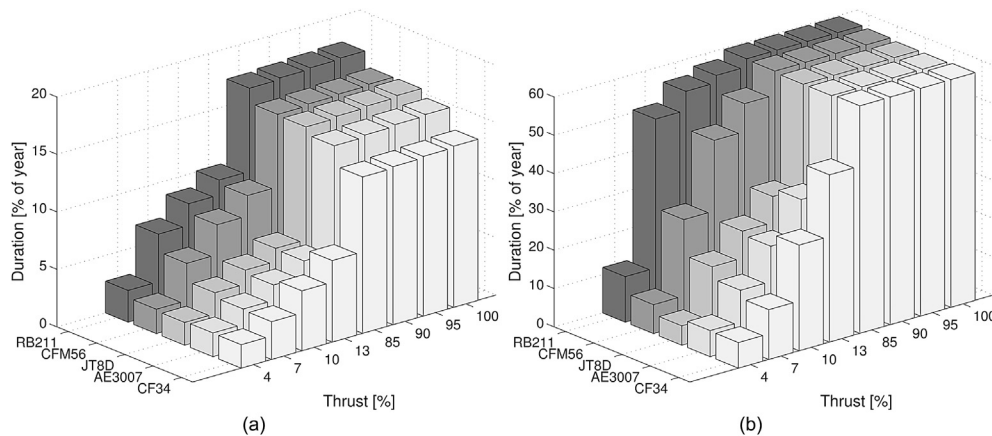
Engine	(Abbrev.)	ICAO UID	Certification	Example aircraft
General Electric CF34-3B	(CF34)	5GE084	1991	Canadair CRJ-200
CFM Int'l. CFM56-7B24	(CFM56)	3CM032	1996	Boeing B737-800
Allison Engine Company AE3007A1	(AE3007)	6AL005	1994	Embraer ERJ-145
Rolls Royce RB211-535E4B	(RB211)	3RR034	1984	Boeing B757-200
Pratt & Whitney JT8D-219	(JT8D)	1PW019	1983	McDonnell Douglas MD88

**Table 2**  
Change in population exposure to PM<sub>2.5</sub> and O<sub>3</sub>, per unit fuel burn at Atlanta's Hartsfield-Jackson airport (ATL). Values are shown for one specific hour (1500–1600 UTC on Jan 10, 2006) and annual average for the RB211 and CFM56 engines. Engine operation is assumed to be at one of the eight thrust settings studied: four taxi thrust settings (4, 7, 10 and 13%) and four takeoff thrust settings (85, 90, 95 and 100%).

$\partial P/\partial F$	PM <sub>2.5</sub> exposure [ppm ngm <sup>-3</sup> kg <sup>-1</sup> ]								
		4%	7%	10%	13%	85%	90%	95%	100%
Jan 10, 2006, 1500 UTC	RB211	0.003	-0.01	-0.02	-0.02	-0.27	-0.30	-0.33	-0.36
	CFM56	0.02	-0.01	-0.02	-0.03	-0.14	-0.15	-0.16	-0.17
Annual average	RB211	0.12	0.15	0.17	0.20	1.36	1.49	1.63	1.78
	CFM56	0.24	0.21	0.23	0.24	0.75	0.79	0.83	0.87

$\partial P/\partial F$	O <sub>3</sub> exposure [ppm ppt kg <sup>-1</sup> ]								
		4%	7%	10%	13%	85%	90%	95%	100%
Jan 10, 2006, 1500 UTC	RB211	0.04	-0.17	-0.24	-0.30	-2.65	-2.94	-3.22	-3.51
	CFM56	0.41	-0.11	-0.25	-0.34	-1.44	-1.52	-1.60	-1.67
Annual average	RB211	0.40	0.33	0.38	0.46	3.61	3.99	4.37	4.77
	CFM56	1.28	0.65	0.57	0.57	1.78	1.87	1.97	2.06



**Fig. 1.** Annual duration of tradeoff, expressed as a fraction of the year, between fuel burn and population exposure to (a) PM<sub>2.5</sub> and (b) O<sub>3</sub>, by each engine type and thrust setting. For each engine and thrust setting, annual durations are averaged over all the 34 airports.

20 to ~53 and  $EI_{NO_x}/EI_{SO_2}$  from ~2.4 to ~22. This trend holds for all other engines. As a result, tradeoff conditions are more dependent on  $S_{NO_x}$  at high thrust settings relative to low thrusts. As  $EI_{NO_x}$  is a positive quantity, the atmospheric sensitivities of PM<sub>2.5</sub> and O<sub>3</sub> exposures to NO<sub>x</sub> have to be negative for  $\partial P/\partial F < 0$  (as will be discussed further in Section 3.1.2). At takeoff thrusts, therefore, the fractions of the year that tradeoff conditions occur for all engines (14–18% for PM<sub>2.5</sub> and ~60% for O<sub>3</sub> exposures, as seen in Fig. 1) approximately equals the annual duration of negative NO<sub>x</sub> sensitivity (~19% for PM<sub>2.5</sub> exposure and 60% for O<sub>3</sub> exposure at all airports).

We observe that engine operations at maximum thrust result in CO<sub>2</sub> emissions – O<sub>3</sub> exposure tradeoff conditions 5–12 times more frequently than operations at 4% thrust. This suggests that minimizing fuel burn during taxi operations is less likely to result in an O<sub>3</sub> exposure tradeoff than reducing fuel burn at takeoff. To explain this, we note that over all airports, engines and thrust settings, less than 5% of the magnitude of CO<sub>2</sub>–O<sub>3</sub> exposure tradeoff is attributable to CO emissions, while <0.4% of the magnitude of CO<sub>2</sub>–O<sub>3</sub> exposure tradeoff is attributed to SO<sub>2</sub> emissions. We therefore simplify Eq. (6) as.

$$\frac{\partial P}{\partial F} \approx S_{NO_x} \cdot EI_{NO_x} + S_{HC} \cdot EI_{HC}. \quad (7)$$

Taking the CFM56 engine as an example, at 100% thrust,  $EI_{NO_x}$  is ~256 times larger than the  $EI_{HC}$  for the CFM56 engine. In order to

create a tradeoff between fuel burn (CO<sub>2</sub> emissions) and population exposure,  $\partial P/\partial F$  has to be less than zero and it follows from Eq. (7) that the condition

$$S_{NO_x} < - (1/256) \cdot S_{HC} \quad (8)$$

must be satisfied. At the 4% thrust setting,  $EI_{HC}$  is ~3 times as larger than that of NO<sub>x</sub> for the CFM56 engine. For tradeoff conditions to occur in this regime, the inequality

$$S_{NO_x} < - 3S_{HC} \quad (9)$$

must be fulfilled. For a given  $S_{HC}$ , atmospheric NO<sub>x</sub> sensitivities must be ~770 times more negative to create tradeoff conditions at 4% thrust than to do so at 100% thrust. Conversely, for a given negative  $S_{NO_x}$ , atmospheric sensitivity to HC should be relatively smaller in magnitude or negative. Over all airports, the combination of sensitivities required to satisfy Eq. (9) occurs less frequently than the occurrence of negative NO<sub>x</sub> sensitivities (~8.6 times less frequently, in the case of the CFM56 engine). As a result, for the CFM56 engine, O<sub>3</sub> exposure tradeoff conditions occur ~8 times less frequently at the 4% thrust setting relative to the 100% setting.

Engine operations at maximum thrust result in CO<sub>2</sub> emissions – PM<sub>2.5</sub> exposure tradeoff conditions 6–8 times more frequently than operations at 4% thrust. Compared to tradeoffs between CO<sub>2</sub> emissions and O<sub>3</sub> exposure, SO<sub>2</sub> emissions contribute to a larger

percentage of the magnitude of CO<sub>2</sub> emissions – PM<sub>2.5</sub> exposure tradeoff (up to 11% for PM<sub>2.5</sub> c.f. <0.4% for O<sub>3</sub>, over all airports and engines). PM<sub>2.5</sub> concentrations have been observed to increase with a reduction in sulfates under ammonia-rich conditions, due to a transfer of nitric acid from the gas phase to the aerosol phase (West et al., 1999). While Eqs. (7)–(9) do not include the contribution of SO<sub>2</sub> emissions to population exposure, they qualitatively describe the trends in PM<sub>2.5</sub> tradeoff duration across thrust settings. For the CFM56 engine, the inequality in Eq. (9) is satisfied less frequently than the occurrence of negative PM<sub>2.5</sub> exposure sensitivity to NO<sub>x</sub> (~9 times less frequently, for the CFM56 engine), which is congruent with durations of tradeoff between CO<sub>2</sub> emissions and PM<sub>2.5</sub> exposure occurring ~7.7 times less frequently at 4% thrust than at 100% thrust.

The duration of tradeoff between CO<sub>2</sub> emissions and population exposure to PM<sub>2.5</sub> and O<sub>3</sub> also varies according to time of year (see Section S4 of the SI) and across airport locations (see Section S5 of the SI for a spatial map).

### 3.1.2. Negative sensitivity of PM<sub>2.5</sub> and O<sub>3</sub> exposure to NO<sub>x</sub>

Negative PM<sub>2.5</sub> and O<sub>3</sub> exposure sensitivity to NO<sub>x</sub> emissions is an important determinant in the occurrence of tradeoff conditions as discussed in Section 3.1.1. Negative sensitivity of O<sub>3</sub> concentrations with NO<sub>x</sub> occurs in a VOC-limited atmosphere (Seinfeld and Pandis, 2006). In this regime, NO<sub>2</sub> oxidizes faster than VOCs. The enhanced oxidation of NO<sub>x</sub> to nitric acid consumes OH and as a result may inhibit oxidation of other PM<sub>2.5</sub> precursors and reduce the mass of secondary PM<sub>2.5</sub> (Megaritis et al., 2013).

Reductions in sulfate aerosols due to NO<sub>x</sub> emissions have been observed in Ashok et al. (2013), Zhang and Wu (2013) and Pinder et al. (2008). The behavior is attributed to competition for free ammonia in the atmosphere. Thus, growth in nitrate aerosol mass due to oxidation of NO<sub>x</sub> may be offset by the reduction in other PM<sub>2.5</sub> components, and a shift in the spatiotemporal pattern of concentrations, thereby leading to reduced PM<sub>2.5</sub> exposure overall in some conditions.

## 3.2. Magnitude of CO<sub>2</sub> emissions – air quality tradeoff

In this section we quantify the magnitude of tradeoff between CO<sub>2</sub> emissions and population exposure to PM<sub>2.5</sub> and O<sub>3</sub>. For a given airport and time of emissions, population exposure is affected by engine operation in two ways: total fuel consumed and thrust setting (see Eq. (5)) – the two main factors controlling emissions.

First, we present the reduction in population exposure to PM<sub>2.5</sub> and O<sub>3</sub> per kilogram increase in fuel burn at constant thrust during tradeoff conditions. Second, we quantify the relationship between thrust setting and population exposure, as in some operational cases thrust setting can be altered. Finally, airports are ranked according to their exposure reduction potentials, i.e. the combination of magnitude and duration of tradeoff between CO<sub>2</sub> emissions and population exposure to PM<sub>2.5</sub> and O<sub>3</sub>.

### 3.2.1. Tradeoff between CO<sub>2</sub> emissions at constant thrust and air quality impacts

The distribution of PM<sub>2.5</sub> and O<sub>3</sub> population exposure reductions per kilogram fuel burned at constant thrust is shown in Fig. 2(a) and (b), respectively. As an example, 1 kg of fuel burned by an RB211 engine at 7% thrust causes a median [25th–75th percentile] reduction in PM<sub>2.5</sub> population exposure of 1.21 [0.33–3.64] × 10<sup>-2</sup> ppl ngm<sup>-3</sup> across all 34 airports during tradeoff conditions.

At 7% thrust, the median reductions in PM<sub>2.5</sub> exposure per kilogram fuel burn is ~0.016 ppl ngm<sup>-3</sup> kg<sup>-1</sup> for all engines, while at 100% thrust the reductions are greater in magnitude and relatively more varied between 0.06 and 0.27 ppl ngm<sup>-3</sup> kg<sup>-1</sup> across the five engines. This trend is also observed in O<sub>3</sub> exposure reductions, which are ~0.25 ppl ppt kg<sup>-1</sup> at 7% thrust and 0.98–4.44 ppl ppt kg<sup>-1</sup> at 100% thrust. Relative to the annual average (positive) PM<sub>2.5</sub> exposure per unit fuel burn, the median reductions in population exposure to PM<sub>2.5</sub> during tradeoff conditions at 7% and 100% thrust are 6–8% and 11–13% respectively, depending on the engine. For O<sub>3</sub> exposure, the relative magnitudes are 32–1060% and 265–314% for fuel burn at 7% and 100%, respectively. The large variability in relative magnitudes across engines means that the potential improvements in O<sub>3</sub> exposure at airports, though significant relative to the annual average, may be sensitive to the fleet composition of airport traffic.

The variation in magnitude of tradeoff at 100% thrust (gray bars in Fig. 2) amongst the engines is explained by differences in the NO<sub>x</sub> EI. At high thrusts reductions in population exposure are more sensitive to variations in EI<sub>NO<sub>x</sub></sub> than other species, in part as EI<sub>NO<sub>x</sub></sub> exceeds that of other species by 1–2 orders of magnitude. Thus for a given (negative) atmospheric sensitivity to NO<sub>x</sub>, engines with larger EI<sub>NO<sub>x</sub></sub> lead to relatively greater reductions in population exposure to O<sub>3</sub> and PM<sub>2.5</sub> per unit fuel burn, than engines with smaller EI<sub>NO<sub>x</sub></sub>. This means that the tradeoff is greater for older engines and engines with higher pressure ratios, in general.

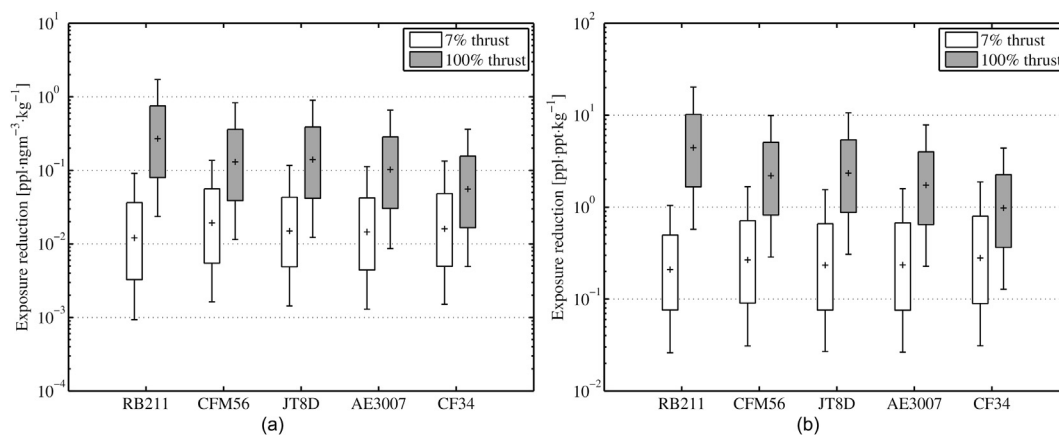


**Fig. 2.** Reduction in population exposure to (a) PM<sub>2.5</sub> and (b) O<sub>3</sub> due to 1 kg of (additional) fuel burned at a constant thrust setting of 7% (white bars) and 100% (gray bars). The marker within the box plot for each engine represents the median value across all airports and tradeoff durations; the box extents are the interquartile range; and the whiskers, the 10th and 90th percentile values.

**Table 3**  
Change in PM<sub>2.5</sub> exposure per unit fuel burn increased due to thrust setting, for the RB211 engine at the ATL airport on 1 Jan 2006, 0600–0700 UTC. Units are ppl ngm<sup>-3</sup> kg<sup>-1</sup>. Changes in population exposure and fuel burn are calculated between each consecutive pair of thrust settings.

Thrust setting range	4%–7%	7%–10%	10%–13%	85%–90%	90%–95%	95%–100%
$\Delta P/\Delta F$ (ppl ngm <sup>-3</sup> kg <sup>-1</sup> )	-0.058	-0.049	-0.059	-0.57	-0.62	-0.68

### 3.2.2. Negative thrust setting – air quality relationship

The operating thrust setting of an engine influences population exposure via two pathways. Firstly, thrust setting affects emission indices and consequently the value of  $\partial P/\partial F$ , as shown in Eq. (6) and Table 2. The second pathway is by affecting fuel burn itself. Assuming a fixed duration of operation, changing the thrust from some reference condition  $\dot{m}_{f,ref}$  to  $\dot{m}_{f,1}$  scales the reference fuel burn  $F_{ref}$  according to  $F_1 = F_{ref} \cdot \dot{m}_{f,1}/\dot{m}_{f,ref}$ .

Here we assume that changing thrust setting does not influence the duration of operation of the engine on the airport surface. Aircraft taxi times on the airport surface are dependent on congestion levels and limited by safety speed restrictions on taxiways; therefore taxiing at a higher thrust setting may or may not influence operation time. Coupling of thrust setting to airport surface movement modeling, including congestion, to the present study will be the subject of future work. For reduced thrust takeoffs, King and Waitz (2005) calculate a 0.6% net increase in fuel burn per percent reduction in takeoff thrust in the LTO phase, but attribute it to increased airborne climb duration up to 3000 ft (~1 km).

We define the tradeoff between thrust setting and air quality as the condition where there is a monotonic decrease in population exposure with increasing thrust. An example of such a condition is shown in Table 3, which tabulates the gradient of PM<sub>2.5</sub> exposure with respect to fuel burn,  $\Delta P/\Delta F$ , between successive thrust settings at ATL. All gradients are negative, implying that population exposure is progressively lowered as thrust setting is increased for a constant operation time. Furthermore, population exposure depends nonlinearly on thrust, as gradients in the takeoff (85–100%) thrust regime are an order of magnitude larger than those in the taxi (4–13%) thrust regime. The nonlinearity arises from the power-law trends of NO<sub>x</sub>, HC and CO EIs with thrust.

We quantify the reduction in population exposure from fuel burn (and CO<sub>2</sub> emissions) increase via thrust setting by computing an average gradient over the taxi and takeoff thrust regimes separately. Over all airports and engine types, negative trends

between thrust and population exposure to PM<sub>2.5</sub> and O<sub>3</sub> occur 13% and 59% of the year, respectively.

PM<sub>2.5</sub> and O<sub>3</sub> exposure reductions per kilogram fuel burn (or per 3.16 kg of CO<sub>2</sub> emissions) increased via thrust setting are shown in Fig. 3(a) and (b). Median PM<sub>2.5</sub> exposure reductions (over all airports) for the five engines are 0.05–0.10 ppl ngm<sup>-3</sup> kg<sup>-1</sup> for thrust changes within the taxi thrust regime, and 0.10–0.78 ppl ngm<sup>-3</sup> kg<sup>-1</sup> for changes in thrust over the takeoff thrust regime. These are 15–54% and 15–23% of the annually averaged change in PM<sub>2.5</sub> exposure per kilogram fuel burn increased via thrust setting, over the taxi and takeoff thrust regimes respectively. Median ozone reductions are 0.80–1.77 ppl ppt kg<sup>-1</sup> and 1.42–8.59 ppl ppt kg<sup>-1</sup> for thrust increments in the taxi and takeoff regimes, respectively. These reductions are 114–218% and 263–320% of the corresponding annually averaged changes in O<sub>3</sub> exposure.

For all except the CF34 engine, increasing fuel burn in the takeoff thrust regime causes a greater reduction in exposure than the same increase in the taxi thrust regime. For the CF34 engine, EI<sub>NO<sub>x</sub></sub> grows at a slower rate with respect to thrust than the other engines (e.g. EI<sub>NO<sub>x</sub></sub> at 100% thrust is ~3 times larger than that at 7%, while the ratio is ~15 for the RB211 engine). As a result, the tradeoff magnitudes for the CF34 engine are similar across thrust setting while those of the other engines vary. We also note that the reductions in PM<sub>2.5</sub> and O<sub>3</sub> exposure are both 1.5–6.4 times larger if fuel burn is increased due to thrust as opposed to increased fuel burn at a constant thrust (Section 3.2.1).

### 3.3. Potential for population exposure reduction at airports

We assess the potential for reduction of population exposure to PM<sub>2.5</sub> and O<sub>3</sub> at airports at the cost of increasing CO<sub>2</sub> emissions by considering both the magnitude of tradeoff as well as the frequency of occurrence. An airport with high potential for exposure reduction has a combination of relatively high magnitude of tradeoff for a relatively large fraction of the year, compared to an airport with

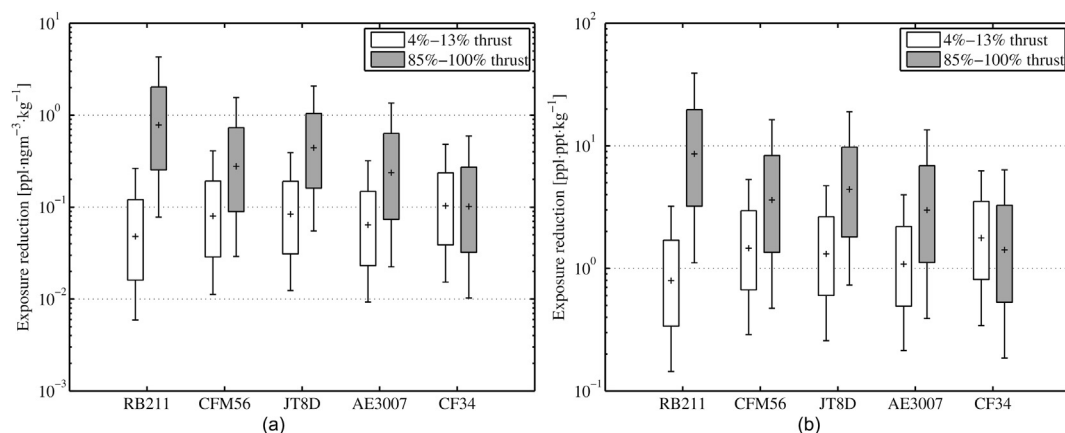


**Fig. 3.** Reduction in population exposure to (a) PM<sub>2.5</sub> and (b) O<sub>3</sub> per kilogram of fuel burn increased via thrust setting, over the taxi thrust (white bars) and takeoff thrust (gray bars) regimes. The marker within the box plot for each engine represents the median value across all airports and tradeoff durations; the box extents, the interquartile range; and the whiskers, the 10th and 90th percentile values.

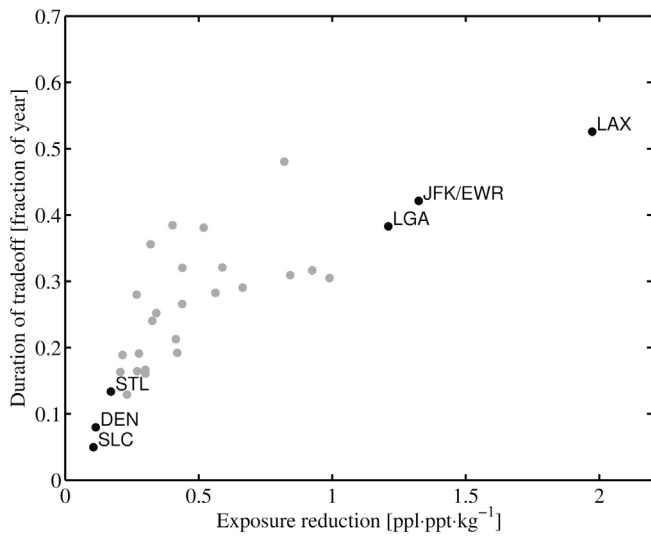


**Fig. 4.** Annual duration of tradeoff plotted against mean O<sub>3</sub> exposure reduction due to 1 kg fuel burn (or 3.16 kg of CO<sub>2</sub> emissions) at 7% thrust for each airport. The three airport locations with the highest and lowest reduction potentials – the product of duration and magnitude of O<sub>3</sub> exposure tradeoff with fuel burn – are highlighted in black and labeled, while all other airports are shown as gray markers and not labeled for clarity.

relatively low exposure reduction potential. Fig. 4 plots the mean reduction in O<sub>3</sub> exposure per kilogram fuel burn at 7% thrust (i.e. taxi operations) against the fraction of the year tradeoff conditions occur, for each airport. The airport locations with the highest and lowest exposure reduction potentials are highlighted and labeled in black. We observe that the Los Angeles (LAX), New York's JFK, Newark (EWR) and La Guardia (LGA) airports have a higher reduction potential relative to the Lambert – St. Louis (STL), Salt Lake City (SLC) and Denver (DEN) airports.

We multiply the average magnitude of tradeoff by the annual duration of occurrence to quantify the PM<sub>2.5</sub> and O<sub>3</sub> exposure reduction potentials at each airport. Reduction potentials are calculated for four engine operation scenarios: increased fuel burn at constant thrust settings of 7% and 100%, as well as thrust increments over the taxi and takeoff thrust regimes. Section S6 of the SI tabulates airport-specific tradeoff magnitudes and annual durations for PM<sub>2.5</sub> and O<sub>3</sub> exposures. The top 5 airports, ranked according to their reduction potentials under each of the four engine operation scenarios, are given in Table 4. The LAX, Philadelphia (PHL) and Cincinnati (CVG) airports are observed to have consistently high PM<sub>2.5</sub> exposure reduction potentials across all four scenarios. For O<sub>3</sub> exposures the LAX, EWR, JFK, LGA and PHL airports have consistently the highest reduction potentials.

#### 4. Conclusions

Aircraft operations on the airport surface contribute to CO<sub>2</sub> emissions that impact the climate and other emissions that affect air quality and human health. Current research efforts on surface movement aim to reduce fuel burn and CO<sub>2</sub> emissions from surface operations, but have not quantified the implication of fuel burn and CO<sub>2</sub> emissions minimization on air quality, and more specifically, population exposure to PM<sub>2.5</sub> and O<sub>3</sub>.

The goal of this work is to identify situations where there is a tradeoff between CO<sub>2</sub> emissions and population exposure to PM<sub>2.5</sub> and O<sub>3</sub> – i.e. conditions when exposure decreases with an increase in fuel burn (directly proportional to CO<sub>2</sub> emissions). The analysis is performed for five commonly-used engines in the US

**Table 4** Top five airports (identified by IATA airport code) ranked by reduction potential, the product of duration and magnitude of CO<sub>2</sub> emissions – exposure tradeoff. Reductions in both PM<sub>2.5</sub> and O<sub>3</sub> exposure are computed for fuel burn increases at constant thrust of 7% and 100%, as well as increases due to thrust setting over the taxi and takeoff thrust regimes. The parenthesis beside each airport lists, in order, the mean magnitude (in ppl ngm<sup>-3</sup> kg<sup>-1</sup> or ppl ppt kg<sup>-1</sup>) and duration (as a fraction of year) of the fuel burn – population exposure tradeoff at that airport. Airports are grouped where they fall in the same –50 km nested GEOS-Chem adjoint grid cell.

Ranking	PM <sub>2.5</sub> exposure reduction				O <sub>3</sub> exposure reduction			
	Increased fuel burn (constant thrust)		Increased thrust		Increased fuel burn (constant thrust)		Increased thrust	
	7%	100%	Taxi range	Takeoff range	7%	100%	Taxi range	Takeoff range
1	LAX (1.58, 0.03)	LAX (3.56, 0.09)	LAX (1.60, 0.08)	LAX (6.76, 0.08)	LAX (1.97, 0.53)	LAX (17.09, 0.83)	LAX (8.36, 0.83)	LAX (28.17, 0.83)
2	PHL (0.14, 0.13)	PHL (0.68, 0.25)	CVG (0.27, 0.30)	PHL (1.21, 0.23)	JFK/EWR (1.32, 0.42)	JFK/EWR (7.20, 0.76)	JFK/EWR (3.39, 0.76)	JFK/EWR (11.86, 0.76)
3	SEA (0.42, 0.03)	SAN (0.48, 0.31)	PIT (0.24, 0.34)	SAN (0.99, 0.25)	LGA (1.21, 0.38)	LGA (6.99, 0.71)	LGA (3.52, 0.71)	LGA (11.50, 0.71)
4	CVG (0.11, 0.08)	CVG (0.46, 0.30)	PHL (0.31, 0.23)	CVG (0.79, 0.30)	BOS (0.82, 0.48)	BOS (4.90, 0.76)	ORD/MDW (2.54, 0.82)	BOS (8.07, 0.77)
5	ORD/MDW (0.12, 0.06)	PIT (0.36, 0.35)	SEA (0.89, 0.05)	PIT (0.65, 0.34)	PHL (0.99, 0.30)	PHL (5.08, 0.67)	PHL (2.75, 0.67)	PHL (8.37, 0.67)

aircraft fleet, and atmospheric conditions at 34 of the 35 OEP airports in the US. Taxi and takeoff thrust levels are modeled. An adjoint approach based on the GEOS-Chem model focused on the North American domain is employed to model secondary PM<sub>2.5</sub> and O<sub>3</sub> population exposure at the regional scale.

A tradeoff between CO<sub>2</sub> emissions and PM<sub>2.5</sub> and O<sub>3</sub> population exposure occurs 2–18% and 5–60% of the year respectively, aggregated across all airport locations and depending on thrust setting. Relative to engine operation at 4% thrust, operations at maximum thrust lead to tradeoff conditions between CO<sub>2</sub> and population exposure to PM<sub>2.5</sub> and O<sub>3</sub> occurring 6–8 and 5–12 times more frequently.

Median reductions in PM<sub>2.5</sub> exposure per kilogram fuel burn at constant thrust, during tradeoff conditions across all airports, are 0.016–0.27 ppl ngm<sup>-3</sup> kg<sup>-1</sup> depending on engine type and thrust setting. Median O<sub>3</sub> exposure reductions during tradeoff conditions are 0.25–4.44 ppl ppt kg<sup>-1</sup>. Relative to annually averaged reductions in population exposure per unit fuel burn, the reductions in PM<sub>2.5</sub> exposure are 6–13% and the reductions in O<sub>3</sub> exposure are 32–1063%. Reductions in both PM<sub>2.5</sub> and O<sub>3</sub> exposure are 1.5–6.4 times larger if fuel burn is increased via thrust setting as opposed to fuel burn at a constant thrust. During periods of a negative relationship between thrust setting and air quality impact, thrust increments within the takeoff thrust regime cause a greater reduction in population exposure to PM<sub>2.5</sub> and O<sub>3</sub> than thrust increases within the taxi thrust regime, for all except the CF34 engine.

We have identified airports with relatively high population exposure reduction potentials i.e. a combination of high duration and magnitude of CO<sub>2</sub> emissions – population exposure tradeoff. The LAX, PHL and CVG airports have high PM<sub>2.5</sub> exposure reduction potentials, while the LAX, EWR/JFK, LGA and PHL airports have high O<sub>3</sub> exposure reduction potentials, relative to the other airports considered.

We note that the climate impact of aviation is affected not only by CO<sub>2</sub> emissions, but also other emissions that simultaneously impact air quality. For example, the mean global warming potential (GWP) for NO<sub>x</sub> (North America, time horizon of 100 years) is –8.2 (Myhre et al., 2013). For the RB211 engine at takeoff thrust, this results in a (negative) CO<sub>2</sub>-equivalent emission that is ~14% relative to CO<sub>2</sub>. It is, however, out of the scope of this paper to conduct further numerical simulation to quantify the total climate impacts in detail.

We have shown that at the airports and engines studied, there are times during the year where population exposure to both PM<sub>2.5</sub> and O<sub>3</sub> can be improved (in some cases, significantly relative to the annual mean), with an increase in fuel burn. This raises the possibility of reducing the air quality impacts of airports beyond minimizing fuel burn and/or optimizing for minimum net environmental impact (considering air quality and climate together). In the context of airport operations, imminent tradeoff conditions may be identified using real time forecasting of atmospheric sensitivities. Aircraft operations could then be optimized for minimum environmental/air quality impact, while fuel burn minimization strategies may be re-evaluated to avoid increasing the air quality impacts.

## Appendix A. Supplementary data

Supplementary data related to this article can be found at <http://dx.doi.org/10.1016/j.atmosenv.2014.10.024>.

## References

Aardenne, J.V., Dentener, F., Dingenen, R.V., Marmmer, E., Vignati, E., Russ, P., Szabo, L., 2009. Global climate policy scenarios: the benefits and trade-offs for air

- pollution. IOP Conf. Ser. Earth Environ. Sci. 6, 282001. <http://dx.doi.org/10.1088/1755-1307/6/8/282001>.
- Ashok, A., Lee, I.H., Arunachalam, S., Waitz, I.A., Yim, S.H.L., Barrett, S.R.H., 2013. Development of a response surface model of aviation's air quality impacts in the United States. *Atmos. Environ.* 77, 445–452. <http://dx.doi.org/10.1016/j.atmosenv.2013.05.023>.
- Bailis, R., Ezziati, M., Kammen, D.M., 2005. Mortality and greenhouse gas impacts of biomass and petroleum energy futures in Africa. *Science* 308, 98–103. <http://dx.doi.org/10.1126/science.1106881>.
- Balakrishnan, H., Jung, Y., 2007. A framework for coordinated surface operations planning at Dallas-Fort Worth International Airport. In: AIAA Guidance, Navigation, and Control Conference, Hilton Head, SC.
- Balk, D.L., Deichmann, U., Yetman, G., Pozzi, F., Hay, S.J., Nelson, A., 2006. Determining global population distribution: methods, applications and data. *Adv. Parasitol.* 62, 119–156. [http://dx.doi.org/10.1016/S0065-308X\(05\)62004-0](http://dx.doi.org/10.1016/S0065-308X(05)62004-0).
- Barrett, S.R.H., Yim, S.H.L., Gilmore, C.K., Murray, L.T., Kuhn, S.R., Tai, A.P.K., Yantosca, R.M., Byun, D.W., Ngan, F., Li, X., Levy, J.I., Ashok, A., Koo, J., Wong, H.M., Dessens, O., Balasubramanian, S., Fleming, G.G., Pearlson, M.N., Wollersheim, C., Malina, R., Arunachalam, S., Binkowski, F.S., Leibensperger, E.M., Jacob, D.J., Hileman, J.I., Waitz, I.A., 2012. Public health, climate, and economic impacts of desulfurizing jet fuel. *Environ. Sci. Technol.* 46 (8), 4275–4282. <http://dx.doi.org/10.1021/es203325a>.
- Barrett, S.R.H., Britter, R.E., Waitz, I.A., 2010. Global mortality attributable to aircraft cruise emissions. *Environ. Sci. Technol.* 44, 7736–7742. <http://dx.doi.org/10.1021/es101325r>.
- Baughcum, S.L., Tritz, T.G., Herndon, S.C., Pickett, D.C., 1996. Scheduled Civil Aircraft Emission Inventories for 1992: Database Development and Analysis. NASA CR 4722, Appendix D.
- Bey, I., Jacob, D.J., Yantosca, R.M., Logan, J.A., Field, B.D., Fiore, A.M., Li, Q., Liu, H.Y., Mickley, L.J., Schultz, M.G., 2001. Global modeling of tropospheric chemistry with assimilated meteorology: model description and evaluation. *J. Geophys. Res.* 106, 23073–23095. <http://dx.doi.org/10.1029/2001JD000807>.
- Burgain, P., Feron, E., Clarke, J.P., 2009. Collaborative virtual queue: fair management of congested departure operations and benefit analysis. *Air Traffic Control Q.* 17 (2), 195–222.
- Dorbian, C.S., Wolfe, P.J., Waitz, I.A., 2011. Estimating the climate and air quality benefits of aviation fuel and emissions reductions. *Atmos. Environ.* 45, 2750–2759. <http://dx.doi.org/10.1016/j.atmosenv.2011.02.025>.
- Errico, R.M., 1997. What is an adjoint model? *Bull. Am. Meteorol. Soc.* 78, 2577–2591. [http://dx.doi.org/10.1175/1520-0477\(1997\)078<2577:WIAAM>2.0.CO;2](http://dx.doi.org/10.1175/1520-0477(1997)078<2577:WIAAM>2.0.CO;2).
- FAA, 2011. FAA Terminal Area Forecast. Available online at: [http://www.faa.gov/about/office\\_org/headquarters\\_offices/apl/aviation\\_forecasts/taf\\_reports/media/TAF\\_summary\\_report\\_FY20112040.pdf](http://www.faa.gov/about/office_org/headquarters_offices/apl/aviation_forecasts/taf_reports/media/TAF_summary_report_FY20112040.pdf) (accessed 02.02.14.).
- Freeman, O.E., Zerriffi, H., 2012. Carbon credits for cookstoves: trade-offs in climate and health benefits. *For. Chron.* 88, 600–608. <http://dx.doi.org/10.5558/tfc2012-112>.
- Henze, D.K., Hakami, A., Seinfeld, J.H., 2007. Development of the adjoint of GEOS-Chem. *Atmos. Chem. Phys.* 7, 2413–2433. <http://dx.doi.org/10.5194/acp-7-2413-2007>.
- Herndon, S.C., Wood, E.C., Franklin, J., Miake-Lye, R., Knighton, W.B., Babb, M., Nakahara, A., Reynolds, T., Balakrishnan, H., 2012. Measurement of Gaseous HAP Emissions from Idling Aircraft as a Function of Engine and Ambient Conditions. Transportation Research Board (63).
- Hsu, H.-H., Adamkiewicz, G., Andres Houseman, E., Vallarino, J., Melly, S.J., Wayson, R.L., Spengler, J.D., Levy, J.I., 2012. The relationship between aviation activities and ultrafine particulate matter concentrations near a mid-sized airport. *Atmos. Environ.* 50, 328–337. <http://dx.doi.org/10.1016/j.atmosenv.2011.12.002>.
- Hu, S., Fruin, S., Kozawa, K., Mara, S., Winer, A.M., Paulson, S.E., 2009. Aircraft emission impacts in a neighborhood adjacent to a general aviation airport in Southern California. *Environ. Sci. Technol.* 43, 8039–8045. <http://dx.doi.org/10.1021/es900975f>.
- ICAO, 2012. EASA – ICAO Aircraft Engine Emissions Databank. Available online at: <http://easa.europa.eu/environment/edb/aircraft-engine-emissions.php> (accessed 02.02.14.).
- Jung, Y., Hoang, T., Montoya, J., Gupta, G., Malik, W., Tobias, L., Wang, H., 2011. Performance evaluation of a surface traffic management tool for Dallas/Fort Worth International Airport. In: Ninth USA/Europe Air Traffic Management Research and Development Seminar, Berlin, Germany.
- King, D., Waitz, I.A., 2005. Assessment of the Effects of Operational Procedures and Derated Thrust on American Airlines B777 Emissions from London's Heathrow and Gatwick Airports. Partnership for Air Transportation Noise and Emissions Reduction Report no. PARTNER-COE-2005-001.
- Koo, J., Wang, Q., Henze, D.K., Waitz, I.A., Barrett, S.R.H., 2013. Spatial sensitivities of human health risk to intercontinental and high-altitude pollution. *Atmos. Environ.* 71, 140–147. <http://dx.doi.org/10.1016/j.atmosenv.2013.01.025>.
- Koornneef, J., Ramirez, A., van Harmelen, T., van Harsen, A., Turkenburg, W., Faaij, A., 2010. The impact of CO<sub>2</sub> capture in the power and heat sector on the emission of SO<sub>2</sub>, NO<sub>x</sub>, particulate matter, volatile organic compounds and NH<sub>3</sub> in the European Union. *Atmos. Environ.* 44, 1369–1385. <http://dx.doi.org/10.1016/j.atmosenv.2010.01.022>.
- Lack, D.A., Cappa, C.D., Langridge, J., Bahreini, R., Buffaloe, G., Brock, C., Cerully, K., Coffman, D., Hayden, K., Holloway, J., Lerner, B., Massoli, P., Li, S.-M., McLaren, R., Middlebrook, A.M., Moore, R., Nenes, A., Nuaaman, I., Onasch, T.B., Peischl, J.,

- Perring, A., Quinn, P.K., Ryerson, T., Schwartz, J.P., Spackman, R., Wofsy, S.C., Worsnop, D., Xiang, B., Williams, E., 2011. Impact of fuel quality regulation and speed reductions on shipping emissions: implications for climate and air quality. *Environ. Sci. Technol.* 45, 9052–9060. <http://dx.doi.org/10.1021/es2013424>.
- Lyon, T.F., Dodds, W.J., Bahr, D.W., 1979. Determination of the Effects of Ambient Conditions on CFM56 Aircraft Engine Emissions. US EPA Office of Air, Noise and Radiation. Report no. EPA-460/3–79/011.
- MacLean, H.L., Lave, L.B., 2000. Environmental implications of alternative-fueled automobiles: air quality and greenhouse gas tradeoffs. *Environ. Sci. Technol.* 34, 225–231. <http://dx.doi.org/10.1021/es9905290>.
- Megaritis, A.G., Fountoukis, C., Charalampidis, P.E., Pilinis, C., Pandis, S.N., 2013. Response of fine particulate matter concentrations to changes of emissions and temperature in Europe. *Atmos. Chem. Phys.* 13, 3423–3443. <http://dx.doi.org/10.5194/acp-13-3423-2013>.
- Myhre, G., Shindell, D., Breon, F.-M., Collins, W., Fuglestedt, J., Huang, J., Koch, D., Lamarque, J.-F., Lee, D., Mendoza, B., Nakajima, T., Robock, A., Stephens, G., Takemura, T., Zhang, H., 2013. Anthropogenic and natural radiative forcing. In: Stocker, T.F., Qin, D., Plattner, G.-K., Tignor, M., Allen, S.K., Boschung, J., Nauels, A., Xia, Y., Bex, V., Midgley, P.M. (Eds.), *Climate Change 2013: the Physical Science Basis. Contribution of Working Group I to the Fifth Assessment Report of the Intergovernmental Panel on Climate Change*. Cambridge University Press, Cambridge, UK and New York, NY, USA.
- Nikoleris, T., Gupta, G., Kistler, M., 2011. Detailed estimation of fuel consumption and emissions during aircraft taxi operations at Dallas/Fort Worth International Airport. *Transp. Res. Part D Transp. Environ.* 16, 302–308. <http://dx.doi.org/10.1016/j.trd.2011.01.007>.
- Partanen, A.I., Laakso, A., Schmidt, A., Kokkola, H., Kuokkanen, T., Pietikäinen, J.-P., Kerminen, V.-M., Lehtinen, K.E.J., Laakso, L., Korhonen, H., 2013. Climate and air quality trade-offs in altering ship fuel sulfur content. *Atmos. Chem. Phys.* 13, 12059–12071. <http://dx.doi.org/10.5194/acp-13-12059-2013>.
- Pinder, R.W., Dennis, R.L., Bhave, P.V., 2008. Observable indicators of the sensitivity of PM<sub>2.5</sub> nitrate to emission reductions—Part I: derivation of the adjusted gas ratio and applicability at regulatory-relevant time scales. *Atmos. Environ.* 42, 1275–1286. <http://dx.doi.org/10.1016/j.atmosenv.2007.10.039>.
- Ravizza, S., Chen, J., Atkin, J.D., Burke, E., Stewart, P., 2013. The trade-off between taxi time and fuel consumption in airport ground movement. *Public Transp.* 5, 25–40. <http://dx.doi.org/10.1007/s12469-013-0060-1>.
- Schürmann, G., Schäfer, K., Jahn, C., Hoffmann, H., Bauerfeind, M., Fleuti, E., Rappenglück, B., 2007. The impact of NO<sub>x</sub>, CO and VOC emissions on the air quality of Zurich airport. *Atmos. Environ.* 41, 103–118. <http://dx.doi.org/10.1016/j.atmosenv.2006.07.030>.
- Seinfeld, J.H., Pandis, S.N., 2006. *Atmospheric Chemistry and Physics: From Air Pollution to Climate Change*, second ed. John Wiley and Sons, Hoboken, NJ.
- Simaiakis, I., Balakrishnan, H., 2009. Queuing models of airport departure processes for emissions reduction. In: *AIAA Guidance, Navigation, and Control Conference*, Chicago, IL.
- Simaiakis, I., Balakrishnan, H., Khadiolkar, H., Reynolds, T.G., Hansman, R.J., Reilly, B., Ullrich, S., 2011. Demonstration of reduced airport congestion through pushback rate control. In: *Ninth USA/Europe Air Traffic Management Research and Development Seminar*, Berlin, Germany.
- Simone, N.W., Stettler, M.E.J., Barrett, S.R.H., 2013. Rapid estimation of global civil aviation emissions with uncertainty quantification. *Transp. Res. Part D Transp. Environ.* 25, 33–41. <http://dx.doi.org/10.1016/j.trd.2013.07.001>.
- Stettler, M.E.J., Eastham, S., Barrett, S.R.H., 2011. Air quality and public health impacts of UK airports. Part I: emissions. *Atmos. Environ.* 45, 5415–5424. <http://dx.doi.org/10.1016/j.atmosenv.2011.07.012>.
- Tzimas, E., Mercier, A., Cormos, C.-C., Peteves, S.D., 2007. Trade-off in emissions of acid gas pollutants and of carbon dioxide in fossil fuel power plants with carbon capture. *Energy Policy* 35, 3991–3998. <http://dx.doi.org/10.1016/j.enpol.2007.01.027>.
- Unal, A., Hu, Y., Chang, M.E., Talat Odman, M., Russell, A.G., 2005. Airport related emissions and impacts on air quality: application to the Atlanta International Airport. *Atmos. Environ.* 39, 5787–5798. <http://dx.doi.org/10.1016/j.atmosenv.2005.05.051>.
- USEPA, 2011. *The Benefits and Costs of the Clean Air Act from 1990 to 2020*. U.S. EPA Office of Air and Radiation.
- West, J.J., Ansari, A.S., Pandis, S.N., 1999. Marginal PM<sub>2.5</sub>: nonlinear aerosol mass response to sulfate reductions in the Eastern United States. *J. Air Waste Manag. Assoc.* 49, 1415–1424.
- Westerdahl, D., Fruin, S., Fine, P., Sioutas, C., 2008. The Los Angeles International Airport as a source of ultrafine particles and other pollutants to nearby communities. *Atmos. Environ.* 42, 3143–3155. <http://dx.doi.org/10.1016/j.atmosenv.2007.09.006>.
- Wey, C.C., Anderson, B.E., Hudgins, C., Wey, C., Li-Jones, X., Winstead, E., Thornhill, L.K., Lobo, P., Hagen, D., Whitefield, P., Yelvington, P.E., Herndon, S.C., Onasch, T.B., Miake-Lye, R.C., Wormhoudt, J., Knighton, W.B., Howard, R., Bryant, D., Corporan, E., Moses, C., Holve, D., Dodds, W., 2006. Aircraft particle emissions experiment (APEX). NASA, Report No. NASA/TM-2006-214382.
- WHO, 2006. *Health Risks of Particulate Matter from Long-range Transboundary Air Pollution*. Joint WHO/Convention Task Force on the Health Aspects of Air Pollution. World Health Organization, Regional Office for Europe. Report no. E88189.
- WHO, 2008. *Health Risks of Ozone from Long-range Transboundary Air Pollution*. World Health Organization, Regional Office for Europe, Copenhagen.
- Woody, M., Haeng Baek, B., Adelman, Z., Omary, M., Fat Lam, Y., Jason West, J., Arunachalam, S., 2011. An assessment of Aviation's contribution to current and future fine particulate matter in the United States. *Atmos. Environ.* 45, 3424–3433. <http://dx.doi.org/10.1016/j.atmosenv.2011.03.041>.
- Yim, S.H.L., Stettler, M.E.J., Barrett, S.R.H., 2013. Air quality and public health impacts of UK airports. Part II: impacts and policy assessment. *Atmos. Environ.* 67, 184–192. <http://dx.doi.org/10.1016/j.atmosenv.2012.10.017>.
- Zhang, Y., Wu, S.-Y., 2013. Fine scale modeling of agricultural air quality over the Southeastern United States using two air quality models. Part II. *Sensit. Stud. Policy Implic. Aerosol Air Qual. Res.* <http://dx.doi.org/10.4209/aaqr.2012.12.0347>.